
Article:
Manton, J.D., Xiao, Y., Turner, R.D. et al. (2018) ELM : super-resolution analysis of wide-field images of fluorescent shell structures. Methods and Applications in Fluorescence, 6 (3). 037001.

https://doi.org/10.1088/2050-6120/aac28e

TECHNICAL NOTE • **OPEN ACCESS**

ELM: super-resolution analysis of wide-field images of fluorescent shell structures

To cite this article: James D Manton *et al* 2018 *Methods Appl. Fluoresc.* **6** 037001

Methods and Applications in Fluorescence

CrossMark

OPEN ACCESS

RECEIVED
20 December 2017

REVISED
23 April 2018

ACCEPTED FOR PUBLICATION
4 May 2018

PUBLISHED
15 May 2018

TECHNICAL NOTE

ELM: super-resolution analysis of wide-field images of fluorescent shell structures

James D Manton[1], **Yao Xiao**[1], **Robert D Turner**[2], **Graham Christie**[1] and **Eric J Rees**[1]

[1] Department of Chemical Engineering & Biotechnology, University of Cambridge, Cambridge, CB3 0AS, United Kingdom
[2] Krebs Institute, University of Sheffield, Sheffield, S10 2TN, United Kingdom

E-mail: ejr36@cam.ac.uk

Keywords: fluorescence, microscopy, image analysis

Supplementary material for this article is available online

Abstract

It is often necessary to precisely quantify the size of specimens in biological studies. When measuring feature size in fluorescence microscopy, significant biases can arise due to blurring of its edges if the feature is smaller than the diffraction limit of resolution. This problem is avoided if an equation describing the feature's entire image is fitted to its image data. In this paper we present open-source software, ELM, which uses this approach to measure the size of spheroidal or cylindrical fluorescent shells with a precision of around 10 nm. This has been used to measure coat protein locations in bacterial spores and cell wall diameter in vegetative bacilli, and may also be valuable in microbiological studies of algae, fungi and viruses. ELM is available for download at https://github.com/quantitativeimaging/ELM.

Conventional optical microscopy is limited to a resolution of around 200 nm due to the diffraction of light [1]. While there are now myriad super-resolution techniques which beat this limit, these require special and costly microscopes [2–4]. Deconvolution can computationally improve the resolution of confocal microscopy images post-capture, but limited signal-to-noise prevents this from significantly enhancing the resolution [5]. Limited resolution poses a problem when trying to accurately measure small feature sizes using image data, because errors are introduced by diffractive blurring of the specimen's edges. However, we can circumvent this problem by fitting an equation for the specimen's entire image to the image data.

Here we present software for such a post-capture analysis of wide-field microscopy images, which produces super-resolution measurements of shell-like fluorescent specimens, such as bacterial spores, without requiring any additional hardware. This allows us to measure protein location with an accuracy of around 10 nm through a combination of parameter-fitting and single particle averaging, in an approach we term 'ellipsoid localisation microscopy' (ELM). We have previously used this method in studies of spherical and ellipsoidal bacterial spores [6], in which we mapped out some of the proteins comprising the coats of *Bacillus megaterium* and *Bacillus subtilis*. We have now collected our previous analysis scripts into an integrated library and simple graphical user interface, increasing the speed around 30-fold through a combination of parallelisation and optimisation of our fitting procedure. This allows any user to perform super-resolution analyses of spherical, ellipsoidal and cylindrical structures, such as bacterial cell membranes, using conventional fluorescence microscopy.

The ELM software comprises a set of Matlab functions that are called by a graphical user interface. These functions segment a fluorescence microscope image to isolate single specimens and then use non-linear least squares methods to iteratively fit a parametric structure to each candidate (figure 1(a)). The fitted results can be subjected to automated quality control to exclude poor fits and quantify confidence. These results are saved to a spreadsheet for further analysis and can be used to generate super-resolution visualisations of the specimens.

We have previously derived an equation describing the intensity distribution $f_{\text{sphere}}(r)$ in the image of a spherical shell of fluorescent material [6]. This equation is termed the spherical model.

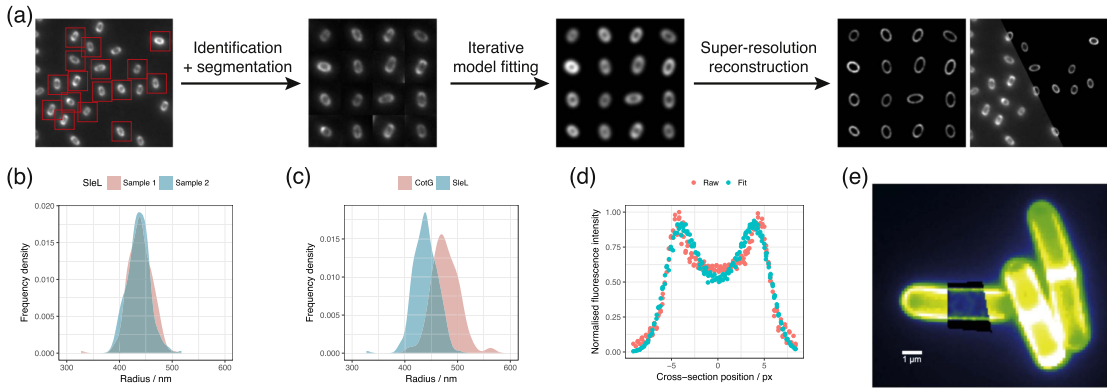

Figure 1. ELM super-resolution analysis as applied to bacterial spore coats and cell walls. (a) The ELM software quantifies the structure of fluorescent shells (such as bacterial spore coats) using a process of segmentation, fitting, and reconstruction. The images of individual shells are automatically identified and then a parametric model for a suitable shell structure (for spheres, ellipsoids) is fitted to each candidate. The fitted parameters provide estimates of protein locations with a precision of about 10 nm, which can then be used to generate a super-resolved image of the specimens. (b), (c) Typically, we image about 500 spores that incorporate a fluorescent fusion protein in their coat. When the same fluorescent coat protein is observed in a second sample of 500 spores, the histogram of estimated protein locations identifies an average radial location for the protein consistent to better than 10 nm, as shown for the SleL-GFP protein in (b). (c) The different locations of distinct coat proteins such as SleL-GFP and CotG-GFP in *B. subtilis* spores can therefore be clearly distinguished despite the separation (30 nm) being far smaller than the diffraction limit of the raw image data. (d) equation (2) provides a model of fluorescence intensity in the image of a cylindrical fluorescent shell (here fluorescent-stained peptoglycan in the cell wall in vegetative *B. subtilis*). Using this model, the ELM software can precisely infer cell wall radius. An excellent fit is obtained between measured pixel data and the model. (e) Using this, super-resolved reconstructions of cylindrical shells can be produced using the same approach as above.

$$f_{\text{sphere}}(r) = aC(e^{-(r-a)^2/2\sigma^2} - e^{-(r+a)^2/2\sigma^2})/r, \quad (1)$$

where r is the radial position with respect to the shell centre, a is the radius of the shell, C is its fluorescence emission per unit area, and σ is the radius of the spherical Gaussian point spread function (PSF) used in the spherical model. All dimensions refer to the specimen space, and derivations are given in (see Supplementary Information available online at stacks.iop.org/MAF/6/037001/mmedia). A cylindrical model for the intensity $f_{\text{cyl}}(D)$ of the image of a thin cylindrical shell at a distance D from the cylinder axis can be obtained using a similar approach.

$$f_{\text{cyl}}(D) = \frac{Ca}{\sigma^2} e^{-(D^2-a^2)/2\sigma^2} I_0\left(\frac{aD}{\sigma^2}\right), \quad (2)$$

where I_0 is the first-order modified Bessel function of the first kind.

An ellipsoidal model provides a better description of the elongated spores more commonly encountered in microbiology, but unfortunately the ellipsoid is harder to analyse. A forward model for the image of an ellipsoidal shell can nonetheless be obtained by numerical summation of the images of a few thousand fluorophores placed randomly on a parametric surface. The image brightness of such a shell at position $\boldsymbol{r}$ is as follows, where (a, b, ψ) are the structural parameters of the shell, h is the PSF of the microscope, and there are N fluorophores randomly located at positions $\boldsymbol{r}_k$ on the shell.

$$f_{\text{ellipsoid}}(\mathbf{r}) = \sum_{k=1}^{N} h(\boldsymbol{r} - \boldsymbol{r}_k(a, b, \psi)) \quad (3)$$

The ellipsoid model involves more parameters and a slower forward image simulation than the spherical model, resulting in slower analysis of image data. However the PSF in the ellipsoid model is no longer constrained to be a spherical Gaussian, and by using a more realistic (ellipsoidal Gaussian) PSF this model provides more accurate fits to real data. Therefore the spherical model can be used to quickly estimate spore structures, but the ellipsoidal model should be used for the most accurate analysis.

Figure 1(a) shows the ELM workflow and typical results when these models are used to infer the structural parameters of vegetative and sporulated *Bacillus* cells. The raw fluorescence micrograph showing several spores is first converted to a tiled image of the computationally-detected spores. Tiled images showing the fitted model parameters and tiled reconstruction with decreased PSF are then shown for comparison. In each case the tiled view is helpful for quality control, as errant fits can be easily spotted and removed from further analyses. Figure 1(b) shows the distribution of protein locations inferred by analysis of two distinct samples using the ellipsoid model, with each sample containing about 500 spores with the same fluorescent protein layer. The protein layer is located, on average, at almost exactly the same location in both samples (438.9 nm and 436.1 nm mean radial location, respectively), demonstrating that the average radius is highly repeatable to better than 10 nm with real spore samples. In figure 1(c), two different protein layers are therefore clearly distinguished by ELM, despite their small separation of 30 nm. Figure 1(d) demonstrates the quality of fit obtained using a cylindrical analysis, as applied to an image of fluorescent-stained peptidoglycan in the bacterial cell

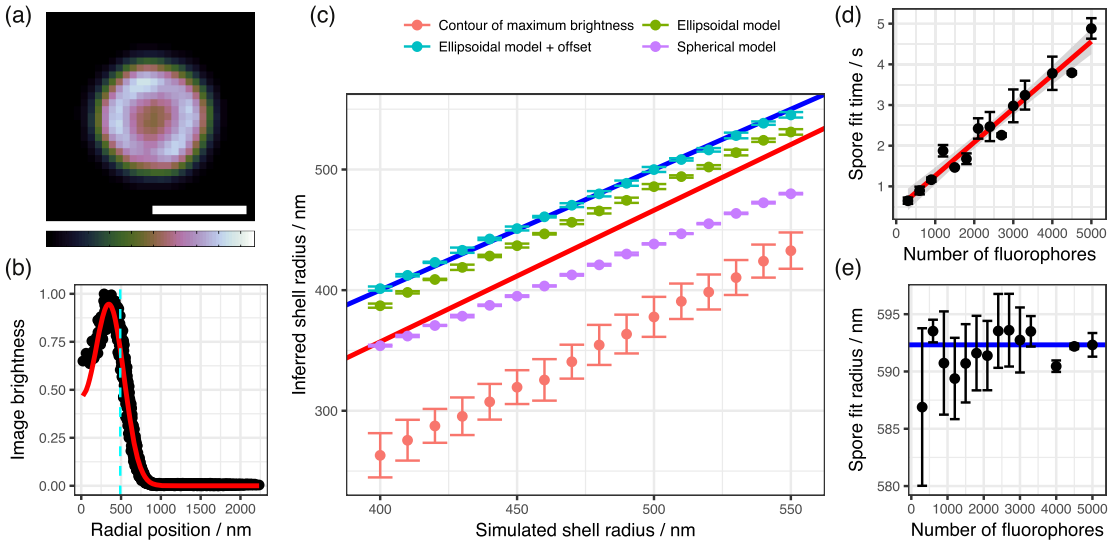

Figure 2. (a) A realistically-simulated image of a spherical spore incorporating a fluorescent protein at a radial location of 490 nm (scale bar 1 μm, cubehelix colourmap [8]). The contour of maximum image brightness is at 370 nm due to diffractive blurring, and is a poor indication of protein location. (b) The idealised image equation (1) provides a fair fit (red) to the data (black), and fitting this equation to the image data provides a much more accurate estimate of the protein location, as shown in (c) (purple markers for spherical model fit compared with the blue line showing the true location and pink markers for the contour of maximum brightness). A still-better estimate of protein location is given by fitting the Monte Carlo model with an ellipsoidal point spread function (green markers), which infers locations with a repeatability better than 5 nm and a small bias of −14 nm with respect to the true location. By adding a fixed offset of +14 nm (cyan markers) the protein location could be recovered to within 5 nm of the true value (blue line), over the entire range of specimen sizes relevant to bacterial spores that is shown here. The protein locations found using the ellipsoid model are far more accurate than the positions indicated by the contour of maximum brightness in the realistically-simulated image data (pink markers), and indeed more accurate than the theoretically-optimal position of the contour of maximum brightness for a microscope with a spherically-symmetric PSF (red line corresponding to equation (4)). (d) When applied to real spore images, the analysis time for the ellipsoid model increases linearly with the number of fluorophores in the model (red line) and remains under 5 s per spore for standard cases on a typical desktop computer. (e) For real spore images the ground truth radial location is unknown, but the precision of the inferred radius with respect to random variation in repeated analyses tends to be better than 10 nm when at least 2000 fluorophores are used in the image model, and it is this random variation rather than the constant offset of about 14 nm that is relevant to studies which seek to distinguish the relative location of different protein layers. The blue line shows the location inferred by a model fit using the largest number of fluorophores in the simulation.

wall, with the corresponding cut-through super-resolution reconstruction shown in figure 1(e).

Figure 2 illustrates the accuracy and speed of the ELM software when applied to both simulated spore images where the ground-truth radius of the specimen is known, and experimental images of spores containing fluorescent coat proteins. First, physically-realistic image data were simulated using TestSTORM software, with structural parameters set to emulate our experimental microscopy of spore coats containing mCherry on an Olympus BX51 wide-field microscope [7]. The contours of maximum brightness in the resulting images always have a radial location much smaller than the true layer radius, due to diffractive blurring. Compared with the ground-truth location of the protein layer, the simple method of measuring the contour of maximum brightness therefore estimates too small a radius. This result could be anticipated from the implicit equation that characterises the turning point of the idealised equation (1), as discussed in the Supplementary Information.

$$e^{2ar/\sigma^2} = \frac{r^2 + ar + \sigma^2}{r^2 - ar + \sigma^2}. \qquad (4)$$

Fitting the idealised spherical image equation also underestimates the radial position of the protein, but by a smaller degree. Furthermore, the radial location parameter inferred from this equation has better linearity and repeatability than the contour of maximum brightness estimator, which means it can correctly distinguish the order of protein layers with smaller separations. Fitting the ellipsoidal model to the simulated image data recovers the protein layer position with repeatability better than 5 nm, and a small constant bias of 14 nm. This allows protein positions to be found very accurately. In practice, the imperfectly spheroidal shape of real spores is likely to prevent much greater accuracy being possible.

In conclusion, we find that the ELM analysis is accurate enough to distinguish protein layer order within the spore coat, and is objectively accurate to within about 15 nm of a protein layer location provided that the protein layer is well approximated as spheroidal. This level of accuracy, combined with the ability to computationally analyse large samples of fluorescence image data, makes ELM a promising new tool for quantitative microbiology that will reveal new maps of bacterial cell walls and spore coats.

Acknowledgments

We gratefully acknowledge support from MedImmune through the Beacon collaboration, from the EPSRC CDT in Sensor Technologies and Applications (EP/L015889/1), and from the BBSRC (BB/L006162/1). We would like to thank Miklos Erdelyi and Tibor Novak for development of TestSTORM, and Mudit Gupta and Alejandro Ayuso-Garcia for preliminary work.

ORCID iDs

James D Manton https://orcid.org/0000-0001-9260-3156

References

[1] Abbe E 1873 Beiträge zur Theorie des Mikroskops und der mikroskopischen Wahrnehmung *Archiv für Mikroskopische Anatomie* **9** 413–68

[2] Hell S W and Wichmann J 1994 Breaking the diffraction resolution limit by stimulated emission: Stimulated-emission-depletion fluorescence microscopy *Opt. Lett.* **19** 780

[3] Betzig E, Patterson G H, Sougrat R, Lindwasser O W, Olenych S, Bonifacino J S, Davidson M W, Lippincott-Schwartz J and Hess H F 2006 Imaging Intracellular Fluorescent Proteins at Nanometer Resolution *Science* **313** 1642–5

[4] Rust M J, Bates M and Zhuang X 2006 Sub-diffraction-limit imaging by stochastic optical reconstruction microscopy (STORM) *Nat. Methods* **3** 793–6

[5] Shaw P 1994 Deconvolution in 3-D optical microscopy *The Histochemical Journal* **26** 687–94

[6] Manetsberger J, Manton J D, Erdelyi M J, Lin H, Rees D, Christie G and Rees E J 2015 Ellipsoid localization microscopy infers the size and order of protein layers in Bacillus spore coats *Biophys. J.* **109** 2058–66

[7] Novák T, Gajdos T, Sinkó J, Szabó G and Erdélyi M 2017 TestSTORM: Versatile simulator software for multimodal super-resolution localization fluorescence microscopy *Sci. Rep.* **7** 951

[8] Green D A 2011 A colour scheme for the display of astronomical intensity images *Bull. Astr. Soc. India* **39** 289–95